Acta Cryst. (1999). A**55**, 933–938

Quantitative phase determination for macromolecular crystals using stereoscopic multibeam imaging

Shih-Lin Chang,[a]* Chun-Hsiung Chao,[a] Yi-Shan Huang,[a] Yuch-Cheng Jean,[b] Hwo-Shuenn Sheu,[b] Fuu-Jye Liang,[a] Hung-Chun Chien,[a] Chun-Kuang Chen[a] and Hanna S. Yuan[c]

[a]*Department of Physics, National Tsing Hua University, Hsinchu, Taiwan 300,* [b]*Synchrotron Radiation Research Center, Hsinchu, Taiwan 300, and* [c]*Institute of Molecular Biology, Academia Sinica, Taipei, Taiwan 115. E-mail: slchang@phys.nthu.edu.tw*

(*Received 11 February 1998; accepted 12 April 1999*)

Abstract

Without invoking anomalous dispersion and heavy-atom derivatives, it is demonstrated that it is possible to directly determine the phases of a large number of reflections collected in a short time from macromolecular crystals using a stereoscopic oscillation-crystal imaging technique, in a multibeam diffraction geometry, where two crystallographic axes in opposite directions are employed as the rotation axes. The intensity profiles (distributions) of the diffraction spots *versus* the varying tilt Bragg angle of the rotation axis in the two stereoscopically related images yield quantitative phase information. Many multiple diffraction profiles of tetragonal lysozyme and an unknown protein structure are obtained at the rate of 100 profiles per 30 min of X-ray exposure.

1. Introduction

The X-ray phase problem is a long-standing important problem in crystallography and X-ray optics. Although the existing mathematical methods, such as direct methods (Ladd & Palmer, 1980; Schenk, 1991; Woolfson & Fan, 1995), multiwavelength anomalous scattering (MAD) (Hendrickson, 1991), and many others (Rossmann, 1972; Bricogne & Gilmore, 1990) are useful phasing techniques for small and macromolecular crystals, the phase problem is not yet completely solved because direct methods run into difficulties with macromolecules since the probability of having the correct phase relation is inversely related to the number of atoms in the crystal unit cell (Ladd & Palmer, 1980) and suitable wavelengths and heavy-atom derivatives may not always be obtainable. Recently, multiple diffraction techniques utilizing interference effects (Post, 1977; Chapman *et al.*, 1981; Chang, 1982; Juretschke, 1982; Hoier & Aanestad, 1981; Hümmer & Billy, 1986; Chang, 1987, and references therein; Mo *et al.*, 1988; Shen & Finkelstein, 1990) have demonstrated their capability of physically measuring reflection phases qualitatively and quantitatively (Chang & Tang, 1988; Weckert & Hümmer, 1990) without invoking multiwavelength experiments and heavy-atom derivatives for macromolecular crystals (Hümmer *et al.*, 1991; Chang *et al.*, 1991; Weckert & Hümmer, 1997, and references therein). Unfortunately, the intensity profiles of multiple diffraction used in phase determination are usually obtained one at a time. The detection of a large collection of diffraction profiles is very difficult because sometimes the crystal deteriorates quickly under X-ray exposure. This fact has seriously hindered this physical technique from becoming practical. In this paper, we consider the enantiomorph (Chang & Tang, 1988; Weckert & Hümmer, 1990) involved in macromolecules and propose a stereoscopic oscillation-crystal imaging technique with multiple diffraction geometry and demonstrate its effectiveness in collecting hundreds of profiles in a short time, thus leading to a quantitative phase-determination method practical for macromolecular crystals (Chang, Chao *et al.*, 1998*a*,*b*).

2. Experimental

Multiple diffraction (MD) takes place when more than one set of atomic planes, say G, L, ..., are simultaneously brought into position to diffract an incident beam (Chang, 1984). For simplicity, consider a three-beam (O, G, L) diffraction, where O stands for the incident beam and G and L are the diffracted beams. In terms of the reciprocal lattice (Fig. 1), three reciprocal-lattice points (r.l.p.'s), O, G and L, are simultaneously on the surface of the Ewald sphere of radius $1/\lambda$, λ being the X-ray wavelength used. Bragg's law is thus satisfied for the three diffracted beams. The vectors **CO**, **CG** and **CL** from the center C of the sphere indicate the directions of the incident and the diffracted beams. If the crystal is rotated around **OG** (the Ψ rotation), other r.l.p.'s like $L_1, L_2, \ldots$ may touch the surface of the Ewald sphere, thus N-beam diffractions $(N > 2)$ such as (O, G, L_1) and (O, G, L_2) occur at different points in time (Fig. 1). At the three-beam (O, G, L) diffraction position, the interaction of the G and L diffracted beams

ISSN 0108-7673

via the coupling $G-L$ reflection within the crystal gives rise to intensity modification on each of the diffracted beams. This modification on the G or L diffracted beam is thus related to the phases of the G, L and $G-L$ reflections or, more precisely, the triplet phases δ_3 $(= \delta_{-G} + \delta_L + \delta_{G-L})$ or δ_3 $(= \delta_{-L} + \delta_G + \delta_{L-G})$ of the structure-factor triplets $F_{-G}F_LF_{G-L}$ or $F_{-L}F_GF_{L-G}$, respectively, provided that the anomalous dispersion is negligibly small (Chang, 1987, and references therein; Weckert & Hümmer, 1997, and references therein). For macromolecular crystals, the three-beam $(O, -G, -L)$ case needs to be used together with the (O, G, L) case to determine their enantiomorphs (Hümmer *et al.*, 1991; Chang *et al.*, 1991). Usually, the multiple diffraction profiles, the intensity I_G *versus* the rotation angle Ψ, of the G reflection are recorded one at a time with a point detector like a scintillation counter (Chang, 1987, and references therein; Weckert & Hümmer, 1997, and references therein). To record the necessary number of MD profiles, simultaneous detection of the diffracted beams at the MD condition is required. In the literature, this has been achieved for a stationary large crystal using a divergent incident beam, the Kossel technique (Kossel, 1936). Many reflection curves from diffraction cones are recorded in a single film. The intersections of conics indicate the occurrence of multiple diffractions (Post, 1977; Post *et al.*, 1977). The intensity modification of MD at the intersection is clearly visualized on the intensity background of the (two-beam) G or L reflection owing to the large beam divergence. It is, however, not the case for tiny organic and macromolecular crystals, because the small crystal size makes the effective beam divergence small. To overcome this difficulty, we propose the following procedure:

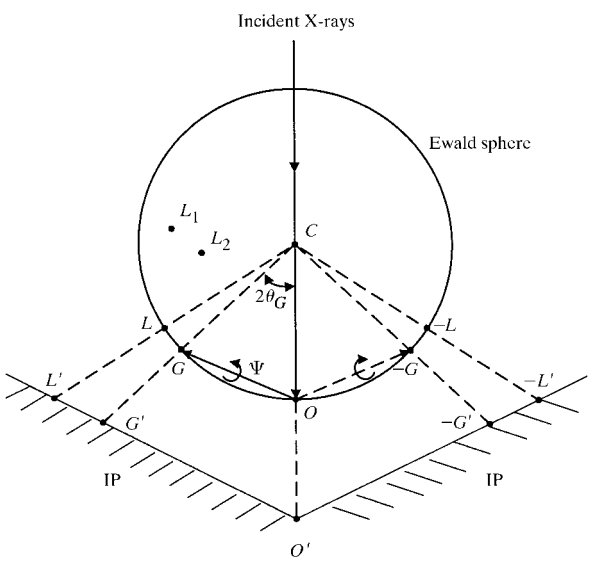

Fig. 1. Diffraction geometry of the stereoscopic multibeam arrangement

From Fig. 1, the crystal is oscillated back and forth in an angular range of $\Delta\Psi$ around **OG** when the r.l.p. of the G reflection (the secondary reflection) is on the surface of the Ewald sphere, *i.e.* $\theta = \theta_G$, θ_G being the Bragg angle of the G reflection. During the oscillation, the r.l.p.'s L, L_1, L_2, ... are brought to cross the surface of the Ewald sphere at different Ψ angles, thus generating the diffracted beams (of the primary reflections L, L_1, L_2, ...), which are recorded in the image plate (IP) set about 10 cm from the crystal and parallel to **OG**. The same intensity recording of the oscillating crystal is repeated on a new IP or on the same IP but shifted by a small $2\Delta\theta$ angle when the crystal is tilted off the Bragg position θ_G by an amount $\Delta\theta$; namely, the r.l.p. G is slightly off the surface of the Ewald sphere, *i.e.* $\theta = \theta_G + \Delta\theta$. Thus, for various θ values, the intensity of the primary reflections within the angular range $\Delta\Psi$ of oscillation are recorded. In other words, the intensity profiles, I_L, I_{L1}, I_{L2}, ..., *versus* $\Delta\theta$, are obtained. The same procedure is taken also for the oscillations around $-$**OG**.

The experiments were carried out on the wiggler beamline SB-05 at the Synchrotron Radiation Research Center (SRRC). The π-polarized incident beam from the 1.86 T 25-pole wiggler with a magnet gap of 22 mm was focused and monochromated by a saggittal Si(111) double-crystal monochromator (SDCM), where the SRRC storage ring was operating at 1.5 GeV and 200 mA. The experimental set-up is similar to that reported by Chang, Huang *et al.* (1998). The beam divergences were 0.01° in the vertical and horizontal directions and $\Delta E/E$ was about 2×10^{-4}. Figs. 2(*a*) and 2(*b*) are the oscillation images ($\Delta\Psi = 2°$) of a lysozyme crystal (tetragonal, unit-cell dimensions $a = b = 78.9$, $c = 38.1$ Å, space group $P4_32_12$; protein data bank entry number 1LYZ) around the $[\overline{1}8,\overline{1}2,1]$ and $[\overline{18},\overline{12},\bar{1}]$ directions (*i.e.* $G = 18,12,1$ and $\overline{18},\overline{12},\bar{1}$) at the peak positions, $\theta_G = \pm 12.263°$ for $\lambda = 1.54228$ Å, respectively. The speed of oscillation is $0.125° \text{ s}^{-1}$, the oscillation range is 2° and the total exposure time for each image is 102 s. The distance between the crystal and the image plate is 10 cm. The mosaic spreads of the crystals investigated are about 0.02–0.04°.

In Figs. 2(*a*) and 2(*b*), all the points, except for (18,12,1) and $(\overline{18},\overline{12},\bar{1})$, are the diffraction spots of the primary reflections satisfying partial or full multiple diffraction interference. Comparison of Fig. 2(*a*) with Fig. 2(*b*) shows that the intensities of some of the primary reflection spots increase or decrease (see *hkl* and $\bar{h}\bar{k}\bar{l}$ spots). Using the software *DENZO* (Otwinowski & Minor, 1997), the integrated intensity of each full primary reflection spot can be read and normalized by the intensity of the incident beam.

Fig. 3 shows the diffracted intensities of the primary reflections of Fig. 2 at various tilt angles $\Delta\theta$ in the vicinity of the secondary reflections (18,12,1) and $(\overline{18},\overline{12},\bar{1})$. The trace of the intensity *versus* $\Delta\theta$ gives the

intensity profile of a given primary reflection. The negative $\Delta\theta$ values correspond to G being outside the Ewald sphere. The same procedure has also been adopted to other secondary reflections, such as 671 and $\bar{6}\bar{7}\bar{1}$.

3. Quantitative phase determination

According to the consideration based on the dynamical theory under the second-order Born approximation for three-beam diffraction (Chang *et al.*, 1991), valid for primary and secondary reflections, the relative intensity, I''_L, of the primary reflection L *versus* the tilt angle $\Delta\theta$ of the secondary reflection G takes the form

$$I''_L = [I_L(3) - I_L(2)]/I_L(2) = I'_L - 1 = I_D + I_K, \quad (1)$$

where the phase-dependent

$$I_D = A[2(\Delta\theta)\cos\delta_3 - \eta\sin\delta_3]/[(\Delta\theta)^2 + (\eta/2)^2]^{1/2} \quad (2)$$

and the phase-independent

$$I_K = AB\{(\eta/2)/[(\Delta\theta)^2 + (\eta/2)^2]\}, \quad (3)$$

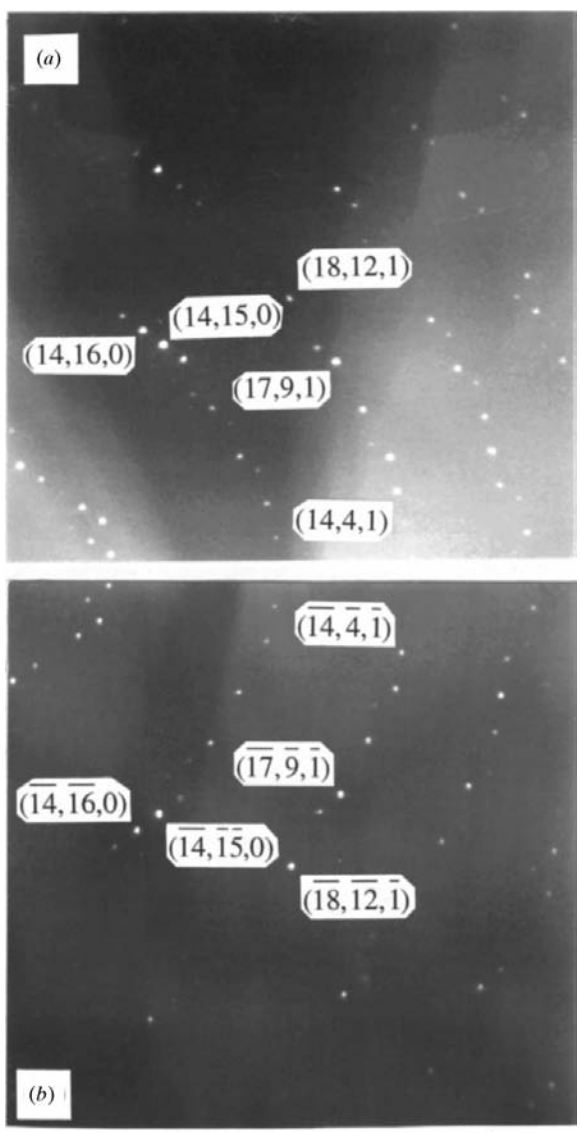

Fig. 2. Stereoscopic images of MD (primary) spots of lysozyme, oscillating around (*a*) [18,12,1] and (*b*) $[\bar{1}\bar{8},\bar{1}\bar{2},1]$ at $\Delta\theta = 0$ and $\lambda = 1.54228$ Å. [All spots can be indexed and the direct beam lies between the (18,12,1) and $(\bar{1}\bar{8},\bar{1}\bar{2},\bar{1})$ spots. The right-angled corner of the labels points to the corresponding spot. Field width: 19° (vertical) and 25° (horizontal).]

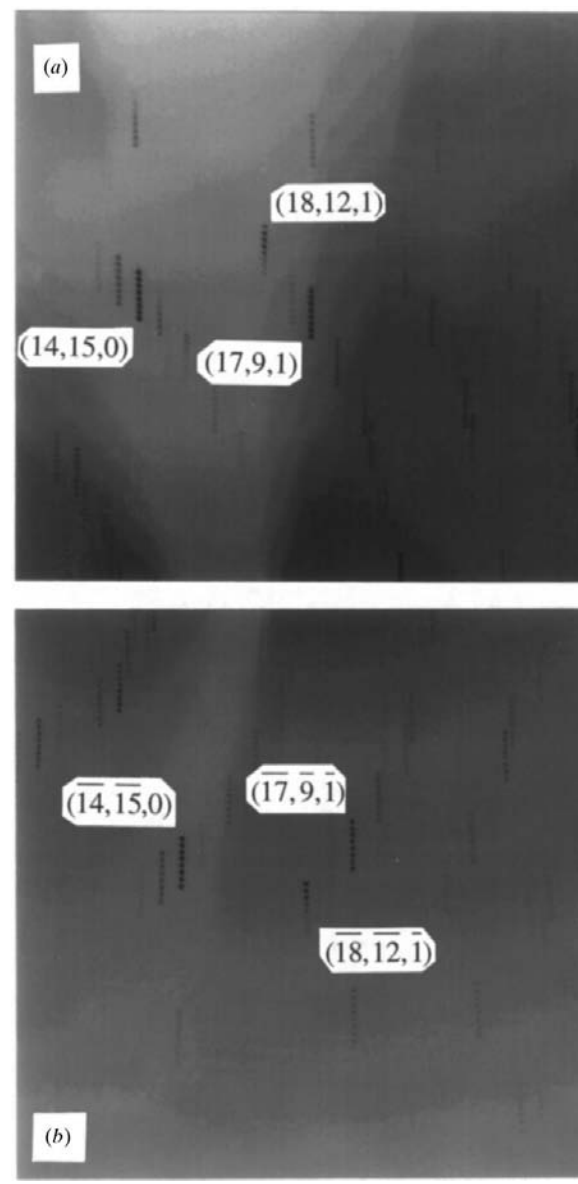

Fig. 3. Stereoscopic images of MD (primary) spots of Fig. 2 at various tilt $\Delta\theta$ angles of the (*a*) 18,12,1 and (*b*) $\bar{1}\bar{8},\bar{1}\bar{2},1$ reflections respectively ($\lambda = 1.54228$ Å).

where η is the peak width at half-maximum. $I_L(2)$ and $I_L(3)$ are the two-beam and three-beam intensities of the L reflection. The quantities A and B depend on the structure-factor moduli and the Lorentz–polarization factor. The corresponding triplet phase is $\delta_3 = \delta_{-L} + \delta_G + \delta_{L-G}$. For the stereoscopic pair (O, G, L) and $(O, -G, -L)$, the δ_3 of the former has the same absolute value but opposite sign to that of the latter without considering anomalous dispersion, because the two cases are centrosymmetrically related. At the exact positions for the G reflection, $\Delta\theta = 0$, the intensity of the case with negative phase values is larger than that with a positive value. For δ_3 close to 0 or 180°, the intensity remains nearly unchanged.

Quantitative determination of the phases δ_3 can be achieved from the intensity profiles of a pair of three-beam cases, (O, G, L) and $(O, -G, -L)$. According to the geometry of generating multiple diffraction, for a given multiple diffraction to occur, there are two positions, IN and OUT, at which the secondary r.l.p. moves towards and leaves the Ewald sphere. To ensure the same X-ray path length in the crystal and extinction for the two symmetry-related three-beam cases, a proper choice of the respective IN and OUT paths must be considered. In the current experiments, a reversal of the X-ray beam paths in the crystal was chosen for the corresponding pairs of multiple diffraction. Figs. 4(*a*) and 4(*b*) show the intensity profiles, the integrated I'_L *versus* $\Delta\theta$, for (14,16,0)/(18,12,1) and $(\overline{14},\overline{16},0)/(\overline{18},\overline{12},1)$ of lysozyme, where the Miller indices L/G are used. According to Chang *et al.* (1991), the triplet phase δ_3 can be determined quantitatively *via*

$$\tan\delta_3 = [-I_+ - I_-]/[I_+ + I_-], \qquad (4)$$

where

$$I_\pm = I_D(\Delta\theta = \pm\eta/2) = I''_L(\Delta\theta = \pm\eta/2) - I_K(\Delta\theta = \pm\eta/2).$$

$I_K(\Delta\theta)$ is a symmetric function of $\Delta\theta$ with the modulus equal to the average value of $I''_L(\Delta\theta = 0)$ of the stereoscopic three-beam pair. The quadrant to which δ_3 belongs is determined by the signs of the numerator and the denominator of (4) (Chang *et al.*, 1991). It should be noted that the determination of the exact position for the G reflection, $\Delta\theta = 0$, can be achieved approximately by minimizing the intensity difference between $I'_L(\Delta\theta = 0)$ and $I'_L(\Delta\theta + \eta/2) + I'_L(\Delta\theta - \eta/2)$ as described by Chang (1998). Following this procedure, the determined phases are $\delta_3 = 77°$ for (14,16,0)/(18,12,1) and −85° for $(\overline{14},\overline{16},0)/(\overline{18},\overline{12},\overline{1})$, compared with the calculated δ_T values 87 and −87°, respectively. The accuracy in δ_3 is within ±20°. For the pair $(\bar{8}\bar{2}6)/(671)$ and $(826)/(\bar{6}\bar{7}\bar{1})$, the MD profiles are shown in Figs. 4(*c*) and 4(*d*). The determined δ_3 is 112° for $(\bar{8}\bar{2}6)/(671)$ and −106° for $(826)/(\bar{6}\bar{7}\bar{1})$, compared with the calculated δ_T values of 100 and −100°. Fig. 5 shows the MD profiles of the pair $(7,\overline{18},5)/(671)$ and $(\bar{7},18,\bar{5})/(\bar{6}7\bar{1})$. The experimentally determined δ_3 are 48 and −40° for the pair, compared with the calculated δ_T values of 31 and −31°, respectively. Other MD profiles for δ_3 close to 0 and 180° are also shown in Fig. 6. The

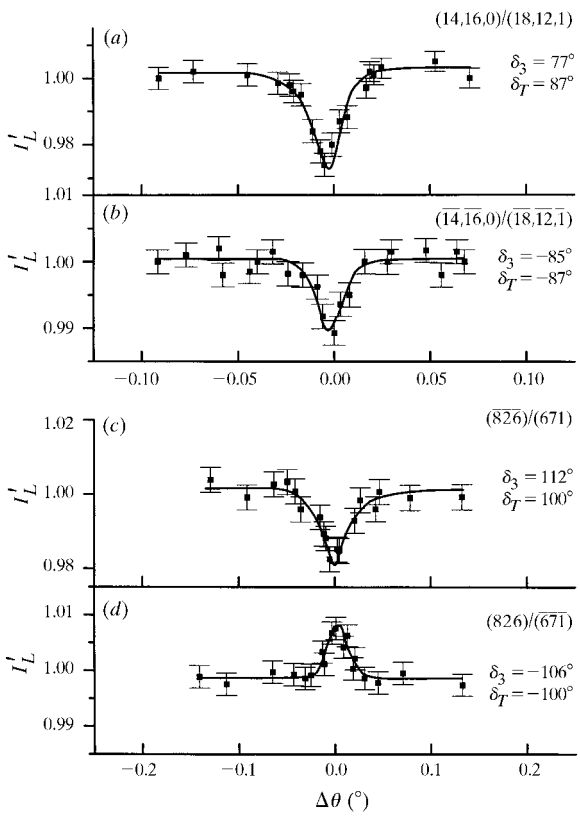

Fig. 4. MD profiles of lysozyme for δ_3 close to ±90° ($\lambda = 1.54228$ Å). The δ_T are the phase values calculated from the known structure.

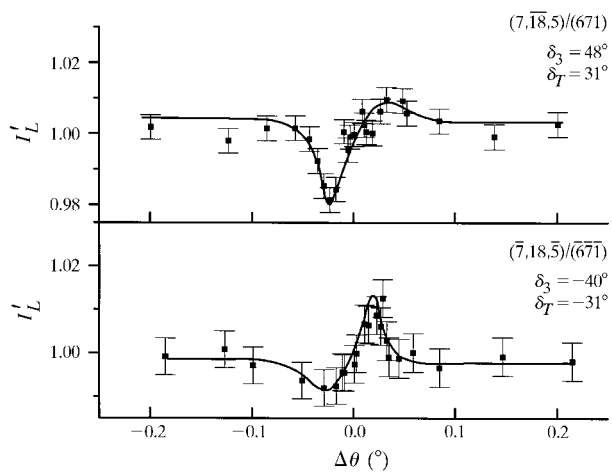

Fig. 5. MD profiles of lysozyme for $\lambda = 1.54228$ Å. The δ_T are the phase values calculated from the known structure.

approximate phase values δ_3 can be deduced from the distinct profile asymmetry, *i.e.* intensity decreasing followed by intensity increasing and *vice versa*. The determined phase values are 7 and -4° for the first pair, *i.e.* $(\bar{1}\bar{0},\bar{6},\bar{7})/(671)$ and $(10,6,7)/(\bar{6}\bar{7}\bar{1})$, and 179 and -178° for the second pair, *i.e.* $(\bar{5}1\bar{4})/(671)$ and $(5\bar{1}4)/(\bar{6}\bar{7}\bar{1})$. The calculated δ_T values are ± 17 and $\pm 174^\circ$, respectively. Similar results can be obtained by inspecting the profile shape proposed by Weckert & Hümmer (1990, 1997, and references therein). We have also applied the present technique to the macromolecular crystal, T2A-Im7 of unknown structure (orthorhombic, $a = 62.3$, $b = 74.8$, $c = 119.6$ Å, space group $I222$), which is the endonuclease domain of colicin E7 complexed with its immunity protein Im7 (Chak *et al.*, 1996). Figs. 7(*a*) and 7(*b*) are the MD profiles of the pair $(5\bar{1}2)/(3\bar{1}2)$ and $(\bar{5}12)/(\bar{3}12)$ of T2A-Im7. The determined δ_3 are 83° for the former and -98° for the latter.

4. Discussion and concluding remarks

We have succeeded in collecting a large number of multiple diffraction profiles by performing a θ–2θ scan for the crystal and using an image plate during the X-ray exposure. The MD profiles showing the intensity asymmetry which conveys phase information are clearly observed for cases involving strong and comparable diffraction strength (*i.e.* large structure-factor moduli) in the G, L and $G-L$ reflections of lysozyme and T2A-Im7. The accuracy in the determined phases is within $\pm 20^\circ$. For the discrimination of the enantiomorph of macromolecular crystals, the use of stereoscopic pairs of multiple diffractions is essential. This in turn leads to quantitative determination of triplet phase invariants. It should be noted that for macromolecular crystals many multiple diffractions occur within 1° of oscillation around the reciprocal-lattice vector of a given G reflection. Only those three-beam and four-beam cases involving strong reflections dominate the diffraction process, thus leading to clear intensity asymmetry ready for phase determination. However, overlapping of strong n-beam cases remains a problem. Up to now, 70% of the collected profiles for the two proteins measured yielded phase information.

In conclusion, we have demonstrated that the collection of a large number of MD profiles useful for phase determination in macromolecular crystals is achieved. The technique proposed thus provides a fast and direct means of phase determination for macromolecular crystals.

If a large number of phases and intensities of unique reflections can be derived from these triplet phases, then the corresponding electron-density map could be derived *via* Fourier transformation. There are, however, many technical problems that have to be overcome, such as how to quickly analyse the vast number of intensity data *versus* $\Delta\theta$, and how to determine the phases of individual reflections from measured triplets. All of these deserve further investigation.

The authors are indebted to the National Science Council for financial support. In preparing this manu-

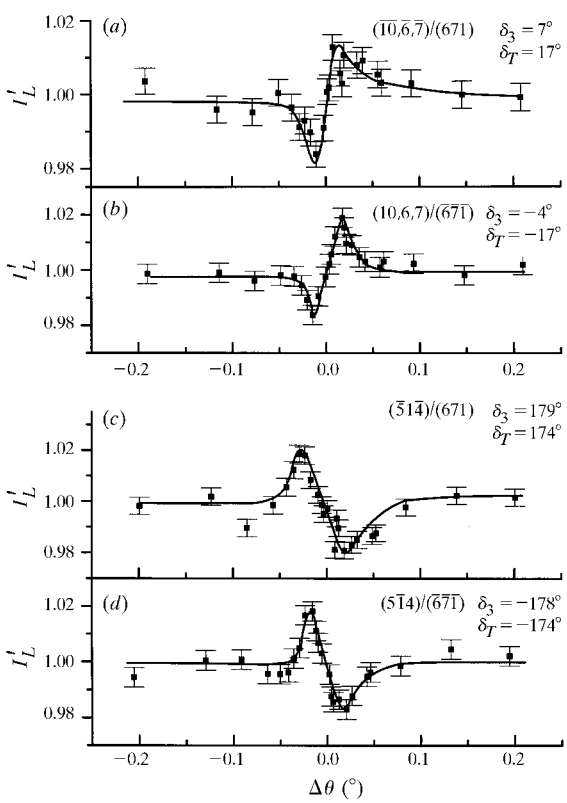

Fig. 6. MD profiles of lysozyme for δ_3 close to 0 and 180° ($\lambda = 1.54228$ Å). The δ_T are the phase values calculated from the known structure.

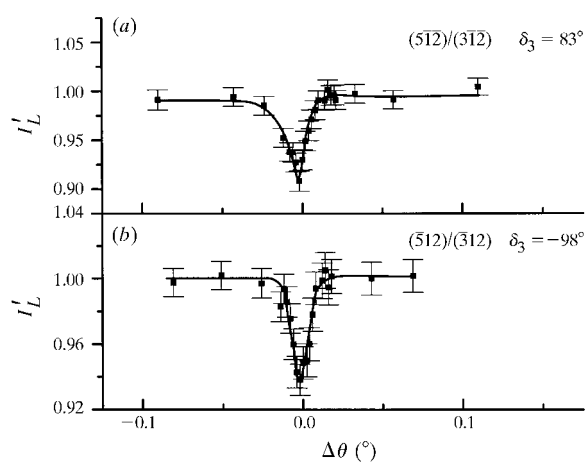

Fig. 7. MD profiles of T2A-Im7 for $\lambda = 1.54228$ Å.

script, we notice that an oscillating-crystal technique for multiple diffraction from a perfect GaAs crystal was reported by Q. Shen (1998).

References

Bricogne, G. & Gilmore, C. J. (1990). *Acta Cryst.* A**46**, 284–297.

Chak, K. F., Safo, M. K., Ku, W. Y., Hsieh, S. Y. & Yuan, H. S. (1996). *Proc. Natl Acad. Sci. USA*, **93**, 6437–6442.

Chang, S. L. (1982). *Phys. Rev. Lett.* **48**, 163–166.

Chang, S. L. (1984). *Multiple Diffraction of X-rays in Crystals.* Berlin: Springer-Verlag.

Chang, S. L. (1987). *Crystallogr. Rev.* **1**, 87–189.

Chang, S. L. (1998). *Acta Cryst.* A**54**, 886–894.

Chang, S. L., Chao, C. H., Huang, Y. S., Jean, Y. C., Sheu, H. S., Liang, F. J., Chien, H. C., Chen, C. K. & Yuan, H. S. (1998*a*). Submitted to *Nature* on 28 February 1998 (unpublished).

Chang, S. L., Chao, C. H., Huang, Y. S., Jean, Y. C., Sheu, H. S., Liang, F. J., Chien, H. C., Chen, C. K. & Yuan H. S. (1998*b*). 3rd Conference of the Asian Crystallogr. Assoc., Bangi, Malaysia, 1998, papers PL-3 and 15P7.

Chang, S. L., Huang, Y. S., Chao, C. H., Tang, M. T. & Stetsko, Y. P. (1998). *Phys. Rev. Lett.* **80**, 301–304.

Chang, S. L., King, H. E., Huang, M. T. & Gao, Y. (1991). *Phys. Rev. Lett.* **67**, 3113–3116.

Chang, S. L. & Tang, M. T. (1988). *Acta Cryst.* A**44**, 1065–1072.

Chapman, L. D., Yoder, D. R. & Colella, R. (1981). *Phys. Rev. Lett.* **46**, 1578–1581.

Hendrickson, W. A. (1991). *Science*, **254**, 51–58.

Hoier, R. & Aanestad, A. (1981). *Acta Cryst.* A**37**, 787–794.

Hümmer, K. & Billy, H. W. (1986). *Acta Cryst.* A**42**, 127–133.

Hümmer, K., Schwegle, W. & Weckert, E. (1991). *Acta Cryst.* A**45**, 60–62.

Juretschke, H. J. (1982). *Phys. Rev. Lett.* **48**, 1487–1490.

Kossel, W. (1936). *Ann. Phys. (Leipzig)*, **26**, 533–553.

Ladd, F. C. & Palmer, R. A. (1980). *Theory and Practice of Direct Methods in Crystallography*. New York: Plenum Press.

Mo, F., Haubach, B. C. & Thorkildsen, G. (1988). *Acta Chem. Scand. Ser. A*, **42**, 130–138.

Otwinowski, Z. & Minor, W. (1997). *Methods Enzymol.* **276**, 307–326.

Post, B. (1977). *Phys. Rev. Lett.* **39**, 760–763.

Post, B., Chang, S. L. & Huang, T. C. (1977). *Acta Cryst.* A**33**, 90–98.

Rossmann, R. G. (1972). Editor. *The Molecular Replacement Method.* New York: Gordon and Breach.

Schenk, H. (1991). Editor. *Direct Methods for Solving Crystal Structures.* New York: Plenum Press.

Shen, Q. (1998). *Phys. Rev. Lett.* **80**, 3268–3271.

Shen, Q. & Finkelstein, K. D. (1990). *Phys. Rev. Lett.* **65**, 3337–3340.

Weckert, E. & Hümmer, K. (1990). *Acta Cryst.* A**46**, 387–393.

Weckert, E. & Hümmer, K. (1997). *Acta Cryst.* A**53**, 108–143.

Woolfson, M. M. & Fan, H.-F. (1995). *Physical and Non-physical Methods of Solving Crystal Structures.* Cambridge University Press.